Multi-Receiver Vector Tracking Based on a Python Platform

Yuting Ng and Grace Xingxin Gao
University of Illinois at Urbana-Champaign

BIOGRAPHY

Yuting Ng is a Master's student in the Aerospace Engineering Department at the University of Illinois at Urbana-Champaign. She received her Bachelor's degree, graduating with university honors, from the Electrical and Computer Engineering Department at the same university in 2014.

Grace Xingxin Gao is an assistant professor in the Aerospace Engineering Department at the University of Illinois at Urbana-Champaign. She obtained her PhD from Stanford University in 2008. She was a research associate at Stanford University from 2008 to 2012.

ABSTRACT

A novel Multi-Receiver Vector Tracking (MRVT) architecture for the joint tracking of multiple GPS receivers to determine the reference position and attitude of a rigid body is presented. The reduction in overall search space, from the state variables of each individual receiver to a single reference position on the rigid body and the attitude of the rigid body, offers increased information redundancy which brings about increased robustness to signal attenuation and multipath. The MRVT architecture is implemented using a Software Defined Radio (SDR) written in Python with an Object-Oriented Programming (OOP) approach that allows easy initialization, modification and extension of the receivers and the multiple receiver network. It also allows for flexible sharing of information at the signal, measurement, data and coordinate levels. Finally, experiments were conducted on a road vehicle for performance evaluation.

I - INTRODUCTION

With the boom of GPS applications such as the navigation of Unmanned Aerial Vehicles (UAVs) and self-driving cars, there is a need for high performance GPS receivers that are robust, accurate and reliable. To meet this need, we aim to leverage on the inherent potential of combining results from more than one receiver for better performance in navigation solution estimation.

We propose a Multi-Receiver Vector Tracking (MRVT) approach, in which we use multiple receivers instead of one receiver to estimate and predict the position of a single reference point on the rigid body and the attitude of the rigid body. Once the position and attitude of the rigid body is determined, the rigid body's state vector is fed-back to each of the individual receivers on the rigid body to augment each of their Vector Tracking Loop (VTL). In this manner, the search space is reduced from the state variables of each individual receiver to the reference position and attitude of the rigid body. This reduction in search space offers increased robustness due to information redundancy.

This paper is organized as follows: Section II describes the theory and implementation of the VTL in each individual receiver. Section III describes the theory and implementation of the Multi-Receiver Vector Tracking Loop (MRVTL). Outputs from the VTL of each individual receiver is used to estimate the state of the MRVTL while the output from the MRVTL is used to augment the VTL of each individual receiver. Section IV describes the experiments that were conducted on a road vehicle. Finally, Section V concludes the paper and provides suggestions for future work.

II – VECTOR TRACKING LOOP

The concept of vector tracking was first proposed by Spilker [1] in 1996 as a Vector Delay Lock Loop (VDLL). Following that, Zhodzishsky et al. [2] extended that concept, with modifications, and created the "Co-OP Tracking for Carrier Phase" where multiple Scalar Phase Lock Loops (SPLLs) and a single Vector Phase Lock Loop (VPLL) run concurrently. Since then, there has been many variations to the idea of vector tracking. Some examples are [3, 4, 5]. In the Joint Vector Tracking Loop of [3], the navigation filter states are not the position, clock bias, velocity and clock drift of the receiver but the amplitude, code phase, code doppler, carrier phase and carrier doppler of each channel. In [4], a Vector Delay and Frequency Lock Loop (VD/FLL) is presented. In [5], the idea of orthogonal projection of tracking error in VPLL, to remove the need for concurrent SPLLs to track channel related errors such as troposphere and ionosphere

errors, is proposed and evaluated. The advances in vector tracking has been nicely summarized in [6]. Finally, the VTL implemented in this paper heavily references [7].

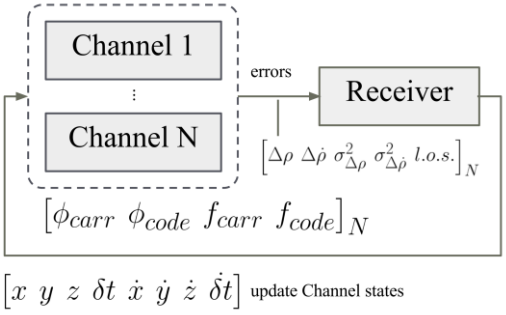

Fig. 1. VTL architecture implemented in this paper

Similar to [7], the non-coherent VTL architecture is implemented in this paper where the input to the navigation filter is the discriminator outputs from each channel. See Fig. 1. The discriminator functions are the normalized early-minus-late power discriminator for VDLL, four quadrant arc-tangent discriminator for VFLL. The discriminator outputs' noise variances are estimated using 300ms sample variances. The VTL is updated every coherent integration period T, 0.001s. The equations are as follows:

$$\Delta\phi_{code} = \frac{E-L}{2(E+L)}, \tag{1a}$$
$$E = \sqrt{iE^2 + qE^2},\ L = \sqrt{iL^2 + qL^2}$$
$$\Delta f_{carrier} = \frac{tan^{-1}(\frac{cross}{dot})}{2\pi T}, \tag{1b}$$
$$cross = iP_0qP_1 - iP_1qP_0,\ dot = iP_0iP_1 + qP_0qP_1$$

$iE, qE, iP, qP, iL, qL =$ in-phase and quadrature-phase early, prompt, late correlations

The discriminator outputs are scaled into pseudorange (m) and pseudorangerate (m/s) errors before being used as inputs to the navigation filter.

$$\Delta\rho = \frac{-c}{f_{C/A}}\Delta\phi_{code} \tag{2a}$$
$$\Delta\dot{\rho} = \frac{-c}{f_{L1}}\Delta f_{carrier} \tag{2b}$$
$\mathcal{C} =$ speed of light, 299792458 (m/s)

The navigation filter within each receiver is an Extended Kalman Filter (EKF). The Kalman correction equations are:

$$K = \widehat{P}H'(R + H\widehat{P}H')^{-1} \tag{3a}$$
$$\Delta x = K\widehat{v} \tag{3b}$$
$$v = H\Delta x \tag{3c}$$
$$x = \widehat{x} + \Delta x \tag{3d}$$
$$P = (I - KH)\widehat{P} \tag{3e}$$

The Kalman prediction equations are:

$$\widehat{x} = Fx \tag{3f}$$
$$\widehat{P} = FPF^{-1} + Q \tag{3g}$$

The state vector x, state transition matrix F, state noise covariance matrix Q, state error covariance matrix P are:

$$x = \begin{bmatrix} x \\ y \\ z \\ \delta t \\ \dot{x} \\ \dot{y} \\ \dot{z} \\ \dot{\delta t} \end{bmatrix} \quad F = \begin{bmatrix} 1 & 0 & 0 & 0 & T & 0 & 0 & 0 \\ 0 & 1 & 0 & 0 & 0 & T & 0 & 0 \\ 0 & 0 & 1 & 0 & 0 & 0 & T & 0 \\ 0 & 0 & 0 & 1 & 0 & 0 & 0 & T \\ 0 & 0 & 0 & 0 & 1 & 0 & 0 & 0 \\ 0 & 0 & 0 & 0 & 0 & 1 & 0 & 0 \\ 0 & 0 & 0 & 0 & 0 & 0 & 1 & 0 \\ 0 & 0 & 0 & 0 & 0 & 0 & 0 & 1 \end{bmatrix}$$

$$Q = P_o = \begin{bmatrix} \sigma_x^2 & 0 & 0 & 0 & 0 & 0 & 0 & \\ 0 & \sigma_y^2 & 0 & 0 & 0 & 0 & 0 & 0 \\ 0 & 0 & \sigma_z^2 & 0 & 0 & 0 & 0 & 0 \\ 0 & 0 & 0 & \sigma_{\delta t}^2 & 0 & 0 & 0 & 0 \\ 0 & 0 & 0 & 0 & \sigma_{\dot{x}}^2 & 0 & 0 & 0 \\ 0 & 0 & 0 & 0 & 0 & \sigma_{\dot{y}}^2 & 0 & 0 \\ 0 & 0 & 0 & 0 & 0 & 0 & \sigma_{\dot{z}}^2 & 0 \\ 0 & 0 & 0 & 0 & 0 & 0 & 0 & \sigma_{\dot{\delta t}}^2 \end{bmatrix}$$

The measurement vector v, measurement projection matrix H, measurement noise covariance matrix R are:

$$v = \begin{bmatrix} \Delta\rho^1 \\ \dots \\ \Delta\rho^n \\ \Delta\dot{\rho}^1 \\ \dots \\ \Delta\dot{\rho}^n \end{bmatrix}$$

$$H = \begin{bmatrix} -los_x^1 & -los_y^1 & -los_z^1 & 1 & 0 & 0 & 0 & 0 \\ \dots & \dots & \dots & \dots & 0 & 0 & 0 & 0 \\ -los_x^n & -los_y^n & -los_z^n & 1 & 0 & 0 & 0 & 0 \\ 0 & 0 & 0 & 0 & -los_x^1 & -los_y^1 & -los_z^1 & 1 \\ 0 & 0 & 0 & 0 & \dots & \dots & \dots & \dots \\ 0 & 0 & 0 & 0 & -los_x^n & -los_y^n & -los_z^n & 1 \end{bmatrix}$$

$$R = \begin{bmatrix} \sigma^2_{\Delta\rho^1} & 0 & 0 & 0 & 0 & 0 \\ 0 & \dots & 0 & 0 & 0 & 0 \\ 0 & 0 & \sigma^2_{\Delta\rho^n} & 0 & 0 & 0 \\ 0 & 0 & 0 & \sigma^2_{\Delta\dot{\rho}^1} & 0 & 0 \\ 0 & 0 & 0 & 0 & \dots & 0 \\ 0 & 0 & 0 & 0 & 0 & \sigma^2_{\Delta\dot{\rho}^n} \end{bmatrix}$$

where the derivation is as follows:

$$\rho^i = \sqrt{(x^i - x)^2 + (y^i - y)^2 + (z^i - z)^2} + b - b^i$$
$$\rho^i = \widehat{\rho^i} - los^i_{x,y,z} \cdot (\Delta x, y, z - \Delta x^i, y^i, z^i) + \Delta b - \Delta b^i$$
$$\therefore \Delta\rho^i = -los^i_{x,y,z} \cdot (\Delta x, y, z - \Delta x^i, y^i, z^i) + \Delta b - \Delta b^i$$

$$\dot{\rho}^i = -los^i_{x,y,z} \cdot (\dot{x}, \dot{y}, \dot{z} - \dot{x}^i, \dot{y}^i, \dot{z}^i) + \dot{b} - \dot{b}^i$$
$$\dot{\rho}^i = \widehat{\dot{\rho}^i} - los^i_{x,y,z} \cdot (\Delta\dot{x}, \dot{y}, \dot{z} - \Delta\dot{x}^i, \dot{y}^i, \dot{z}^i) + \Delta\dot{b} - \Delta\dot{b}^i$$
$$\therefore \Delta\dot{\rho}^i = -los^i_{x,y,z} \cdot (\Delta\dot{x}, \dot{y}, \dot{z} - \Delta\dot{x}^i, \dot{y}^i, \dot{z}^i) + \Delta\dot{b} - \Delta\dot{b}^i$$
$$b = \delta t, \dot{b} = \delta t$$

The errors due to satellite state are assumed to be negligible as changes in satellite state from one navigation epoch to the next are accounted for in the code and carrier replica generation.

The corrected measurement vector v and predicted state vector x-hat are used to update the code and carrier replica generation. The corrected measurement vector v is scaled to reflect the errors in code phase and carrier frequency. It is then used to update the code phase and carrier frequency.

$$\Delta\phi_{code} = \frac{-f_{C/A}}{c}\Delta v_{1\ldots n}, \quad (4a)$$
$$\widehat{\phi_{code}} = \widehat{\phi_{code}} + \Delta\phi_{code}$$
$$\Delta f_{carrier} = \frac{-f_{L1}}{c}\Delta v_{n+1\ldots 2n}, \quad (4b)$$
$$\widehat{f_{carrier}} = \widehat{f_{carrier}} + \Delta f_{carrier}$$
$$\Delta f_{code} = \frac{f_{C/A}}{f_{L1}}\Delta f_{carrier}, \quad (4c)$$
$$\widehat{f_{code}} = \widehat{f_{code}} + \Delta f_{code}$$

The satellite states at the next navigation epoch is then determined. Together with the predicted state vector x-hat, the changes in pseudorange and pseudorangerate are determined. The changes in pseudorange and pseudorangerate are then scaled to reflect the changes in code phase and carrier frequency. It is then used to update the code phase and carrier frequency.

$$\widehat{\Delta\phi_{code}} = \frac{-f_{C/A}}{c}\widehat{\Delta\rho}, \quad (5a)$$
$$\widehat{\phi_{code}} = \phi_{code} + \widehat{\Delta\phi_{code}}$$
$$\widehat{\Delta f_{carrier}} = \frac{-f_{L1}}{c}\widehat{\Delta\dot{\rho}}, \quad (5b)$$
$$\widehat{f_{carrier}} = f_{carrier} + \widehat{\Delta f_{carrier}}$$
$$\widehat{\Delta f_{code}} = \frac{f_{C/A}}{f_{L1}}\widehat{\Delta f_{carrier}}, \quad (5c)$$
$$\widehat{f_{code}} = f_{code} + \widehat{\Delta f_{code}}$$

where the derivation is as follows:
$$\rho^i = c((t+b) - (t^i + b^i))$$
$$\rho^i = c((t+b) - (\Phi^i_{code} + \frac{\phi^i_{code}}{f_{C/A}}))$$
$$\therefore \Delta\rho^i = \frac{-c}{f_{C/A}}\Delta\phi^i_{code}$$
$$\dot{\rho}^i = \frac{-c}{f_{L1}}f_{carrier}$$
$$\therefore \Delta\dot{\rho}^i = \frac{-c}{f_{L1}}\Delta f_{carrier}$$

III – MULTI-RECEIVER VECTOR TRACKING LOOP

In the MRVT architecture, the corrected state vectors of each of the individual receivers, from the same GPS epoch, are used to determine the reference position and attitude of the rigid body. After the reference position and attitude of the rigid body has been determined, it is used to augment the VTL of the individual receivers. See Fig. 2.a. and Fig. 2.b.

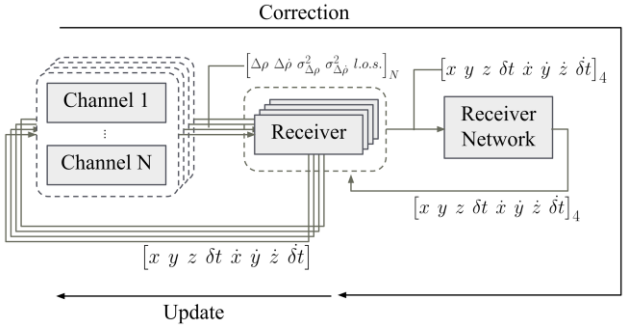

Fig. 2.a. MRVT overall architecture

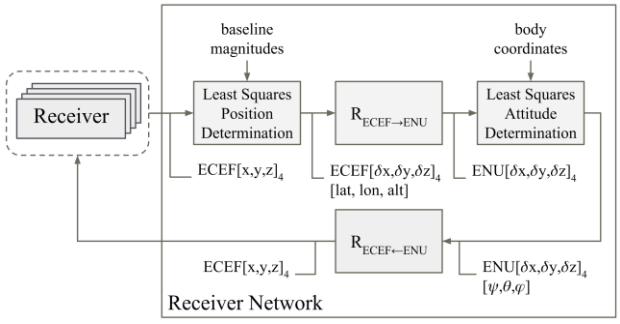

Fig. 2.b. MRVTL implemented in this paper

In addition, individual receivers are synchronized such that their clock bias matches that of the reference clock bias of the receiver network. To achieve this synchronization, the required amount of data samples to be skipped in each individual receiver is estimated during the initialization of the MRVTL using the initial estimate of the receiver state.

In this first iteration of the MRVT architecture, the joint variables being estimated are the x,y,z position parameters of a reference point on the rigid body in the Earth-Centered-Earth-Fixed (ECEF) frame and the yaw, roll, pitch (y, r, p) attitude parameters of the rigid body in the rigid body's local East-North-Up (ENU) frame. The navigation filter is Iterative Least-Squares.

Firstly, using the corrected positions of each of the individual receivers, and prior knowledge of the baseline magnitude with respect to the reference point, the position

of the reference point on the rigid body is estimated. The equations are very similar to the pseudorange equations used in navigation solution estimation. They are derived as follows:

$$b_i = \sqrt{(x_i - x_0)^2 + (y_i - y_0)^2 + (z_i - z_0)^2}$$
$$b_i = \widehat{b_i} - los_{i;x,y,z} \cdot \Delta x_0, y_0, z_0$$
$$\therefore -los_{i;x,y,z} \cdot \Delta x_0, y_0, z_0 = b_i - \widehat{b_i} \quad (6a)$$
$$x_0, y_0, z_0 = \widehat{x_0}, \widehat{y_0}, \widehat{z_0} + \Delta x_0, y_0, z_0 \quad (6b)$$

After the reference position is estimated, the latitude, longitude and altitude (lat, lon, alt) coordinates of the reference position is determined. The corrected positions of each of the individual receivers, relative to the reference position, are then translated and rotated into the local ENU frame of the reference position in preparation for attitude determination. The attitude determination algorithm used in this paper heavily references [8, 9].

Rotation of the position of the individual receivers, relative to the reference position, from ECEF to ENU:

$$\begin{bmatrix} x \\ y \\ z \end{bmatrix}_{ENU} = R_{ENU \leftarrow ECEF} \begin{bmatrix} x - x_0 \\ y - y_0 \\ z - z_0 \end{bmatrix}_{ECEF} \quad (7)$$
$$R_{ENU \leftarrow ECEF} = \begin{bmatrix} -\sin(lon) & \cos(lon) & 0 \\ -\sin(lat)\cos(lon) & -\sin(lat)\sin(lon) & \cos(lat) \\ \cos(lat)\cos(lon) & \cos(lat)\sin(lon) & \sin(lat) \end{bmatrix}$$

Before embarking on the iterative least-squares determination of the attitude, a third coordinate system known as the body coordinates has to be introduced. The body coordinates is an arbitrary coordinate system used to describe the antenna geometry. In this paper, the body coordinates has its origin at the reference position of the rigid body, its x-axis to the right, its y-axis to the front and its z-axis to the top of the rigid body. The relationship between the body coordinates and ENU is described by a rotation matrix:

$$\begin{bmatrix} x \\ y \\ z \end{bmatrix}_{body} = R_{body \leftarrow ENU} \begin{bmatrix} x \\ y \\ z \end{bmatrix}_{ENU} \quad (8)$$
$$R_{body \leftarrow ENU} = \begin{bmatrix} c(r)c(y) - s(r)s(p)s(y) & c(r)s(y) + s(r)s(p)c(y) & -s(r)c(p) \\ -c(p)s(y) & c(p)c(y) & s(p) \\ s(r)c(y) + c(r)s(p)s(y) & s(r)s(y) - c(r)s(p)c(y) & c(r)c(p) \end{bmatrix}$$

where c(.) and s(.) are short-hand notations for cosine(.) and sine(.)

The iterative least-squares equations are then given as equations (2, 3, 4, 5) of reference [9] and will not be repeated here.

After the reference position and attitude of the rigid body has been determined via iterative least-squares, the twice corrected position of each of the individual receivers are then obtained using the body coordinates of each of the individual receivers and the reference position and attitude of the rigid body. This twice corrected position of each of the individual receivers is then fed-back to the each of the individual receivers as the corrected position in the Kalman filter. The Kalman prediction step then follows.

$$\begin{bmatrix} x \\ y \\ z \end{bmatrix}_{ENU} = R'_{body \leftarrow ENU} \begin{bmatrix} x \\ y \\ z \end{bmatrix}_{body} \quad (9a)$$
$$\begin{bmatrix} x \\ y \\ z \end{bmatrix}_{ECEF} = \begin{bmatrix} x_0 \\ y_0 \\ x_0 \end{bmatrix}_{ECEF} + R'_{ENU \leftarrow ECEF} \begin{bmatrix} x \\ y \\ z \end{bmatrix}_{ENU} \quad (9b)$$

In this manner, the search for the position of the individual receivers are constrained by the fixed antenna baselines and geometries. The reduction in the overall search space from the positions of each of the receivers to a single reference position on the rigid body and the attitude of the rigid body offers increased robustness to signal attenuation and multipath.

IV – EXPERIMENTS ON A ROAD VEHICLE

An experiment on a road vehicle was conducted to evaluate the performance of the MRVTL. Four GPS antennas were installed at the four corners of a vehicle's roof. See Fig. 3.a. and Fig. 3.b. Each antenna was connected to a Universal Software Radio Peripheral (USRP). The USRPs are then connected to the same external clock. The USRPs used were USRP N210, each equipped with a DBSRX2 daughterboard, by Ettus Research. The external clock was Quantum SA.45s Chip Scale Atomic Clock by Microsemi. The data were collected through an Ethernet switch and written directly onto the hard disk of a laptop running Ubuntu 12.04. The data was collected as complex short at a sampling frequency of 2.0MHz and at an intermediate frequency of 0MHz. Due to hardware limitiations, there would be a buffer overflow when data is collected at greater sampling frequencies. A power regulating circuit was built to power the equipment from a 12V sealed lead acid battery.

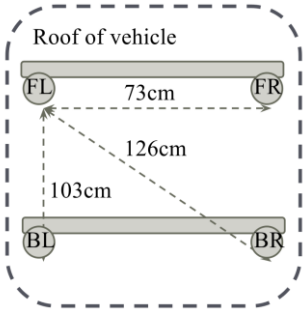

Fig. 3.a. Antenna geometry on the roof of the vehicle

Fig. 3.b. Antennas slightly shifted after data collection

The collected data were processed using our OOP Python SDR which heavily references [10, 11, 12, 13, 14] and our prior work [15]. A simplified block diagram, class diagram and a typical object from our OOP Python SDR are shown in Fig. 4.a., Fig. 4.b. and Fig. 4.c.

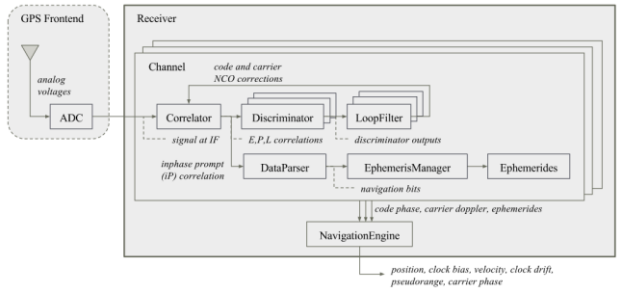

Fig. 4.a. Simplified block diagram of the Python Receiver showing the interaction between the core scalar tracking objects. In this figure, solid triangular arrows represent data being passed from one object to the next.

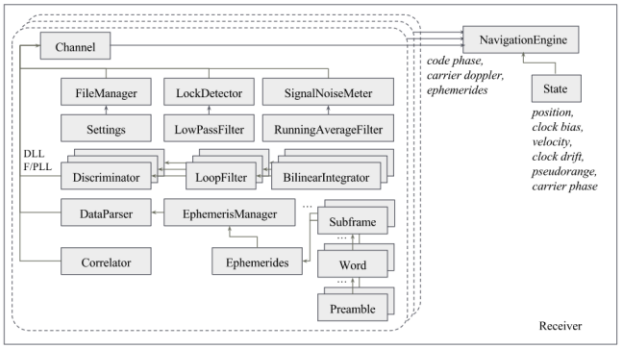

Fig. 4.b. Simplified class diagram of the Python Receiver showing class relationships, to reduce clutter, only "has_a" relationships are shown.

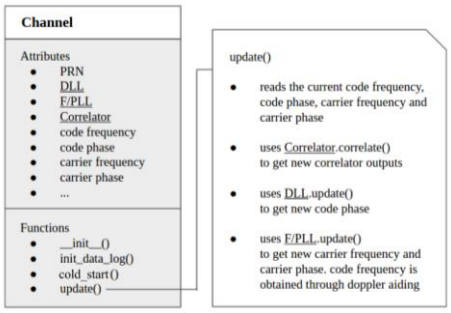

Fig. 4.c. Channel object showing attributes and functions. In addition, the update() function in scalar tracking mode is described.

We processed the data collected with both the single-receiver vector tracking (SRVT) architecture and MRVT architecture. The results are as shown in Fig. 5.a., Fig. 5.b. and Table 1.

Fig. 5.a. Single-receiver vector tracking (SRVT) results of the four GPS antennas installed on the roof of the road vehicle displayed in orange. The vehicle was initially stationary in the parking lot at the bottom right while the receivers are being initialized and synchronized while in scalar tracking mode. The vehicle then turned onto the road and drove north.

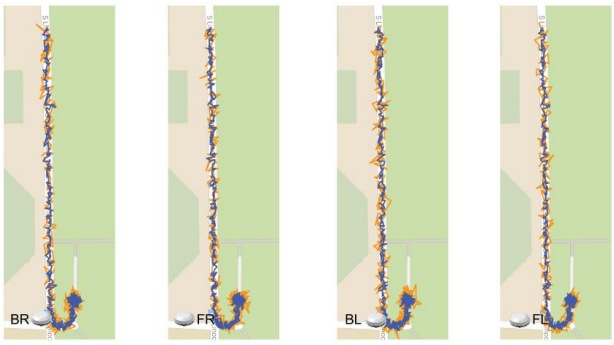

Fig. 5.b. MRVT results of the four GPS antennas installed on the roof of the road vehicle displayed in blue. There is a decrease in noise levels of the results between SRVT and MRVT. For this experiment, the pre-detection integration timing was 1millisecond and there was no additional filter between the discriminators in the channels and EKF in the receiver to reduce noise levels.

As such, the attitude estimates obtained from the receiver coordinates alone were noisy and inaccurate. Instead, prior information of the vehicle moving north was used to provide more accurate attitude estimates.

	SRVT	MRVT
σ(x) (m)	2.93	0.86
σ(y) (m)	4.70	0.86
σ(z) (m)	5.10	0.86
σ(δt) (ns)	15.4	6.73
σ(ẋ) (m/s)	0.31	0.27
σ(ẏ) (m/s)	0.39	0.27
σ(ż) (m/s)	0.45	0.26
σ(δṫ) (ns/s)	1.44	0.82

Table 1. Tabulation of the noise standard deviations of the results obtained from SRVT as compared to MRVT.

V – CONCLUSION AND FUTURE WORK

In conclusion, a MRVT architecture has been proposed as an extension of SRVT. By reducing the search space from the state variables of each individual receiver to the reference position and attitude of the rigid body, the increased information redundancy offers increased robustness to signal attenuation and multipath. In MRVT, we compensated for the receiver timing differences and also performed various coordinate transformations. We implemented an entire SDR based on an OOP approach in the python programming language with the goal of effective information sharing and the added benefits of having a receiver that is intuitive, flexible and extensible. We have also validated the accuracy of our SDR. Next, we conducted experiments, including that on a ground vehicle with four USRPs, one CSAC and our portable power supply. Finally, we validated our MRVT algorithm and demonstrated improved accuracy.

Some future work would be to perform orthogonal projection of the tracking errors in the carrier phase domain and implement a MRVT architecture with phase lock. Another improvement would be to convert the iterative least squares filter used in the MRVTL to an EKF with filter states as position, velocity, attitude and angular velocities.

ACKNOWLEDGMENTS

The author would like to thank Dr. Yu-Hsuan Chen, Enyu Luo, Ganshun Lim, James Jianxiong Kok, Daniel Chou and Athindran Rakesh Kumar for helping with data collection. Dr. Gary McGraw for implementation advice. Akshay Shetty for helping with coordinate transformations. Eliot Wycoff for working on the first iteration of the Python Receiver. Family members, friends, lab members and Prof. Grace Gao for guidance and encouragement.

This paper was partially supported by the Trustworthy Cyber Infrastructure for the Power Grid (TCIPG). The equipment used in producing the results shown in this paper was a courtesy of [16].

REFERENCES

[1] Parkinson, B., & Spilker Jr, J. (1996). *Global Positioning System: Theory and Applications* (Vol. 1, pp. 291-327). Washington, D.C.: American Institute of Aeronautics and Astronautics.

[2] Zhodzishsky, M., Yudanov, S., Veitsel, V., Ashjaee, J., "Co-OP Tracking for Carrier Phase,"*Proceedings of the 11th International Technical Meeting of the Satellite Division of The Institute of Navigation (ION GPS 1998)*, Nashville, TN, September 1998, pp. 653-664.

[3] Liu, J., Cui, X., Chen, Q., Lu, M., "Joint Vector Tracking Loop in a GNSS Receiver," *Proceedings of the 2011 International Technical Meeting of The Institute of Navigation*, San Diego, CA, January 2011, pp. 1025-1032.

[4] Zhao, S., Akos, D., "An Open Source GPS/GNSS Vector Tracking Loop - Implementation, Filter Tuning, and Results," *Proceedings of the 2011 International Technical Meeting of The Institute of Navigation*, San Diego, CA, January 2011, pp. 1293-1305.

[5] Henkel, P., Giger, K., & Gunther, C. (2004). Multifrequency, Multisatellite Vector Phase-Locked Loop for Robust Carrier Tracking. *IEEE Journal of Selected Topics in Signal Processing*, *3*(4), 674-681. Retrieved November 1, 2014, from http://ieeexplore.ieee.org/stamp/stamp.jsp?tp=&arnumber=5166551

[6] Brewer, J. (2014). The Differential Vector Phase-Locked Loop for Global Navigation Satellite System Signal Tracking. *PhD Dissertation*, 22-40. Retrieved August 1, 2014, from http://www.dtic.mil/cgi-bin/GetTRDoc?AD=ADA603126

[7] Bhattacharyya, S. (2012). Performance and Integrity Analysis of the Vector Tracking Architecture of GNSS Receivers. *PhD Dissertation*, 39-114. Retrieved August 1, 2014, from http://www.aem.umn.edu/info/spotlight/bhattacharyya_thesis_final.pdf

[8] Lu, Gang, Lachapelle, Gérard, Cannon, M. Elizabeth, Kielland, Peter, "Attitude Determination in a Survey Launch Using Multi-Antenna GPS Technology," *Proceedings of the 1993 National Technical Meeting of The Institute of Navigation*, San Francisco, CA, January 1993, pp. 251-259.

[9] Dai, Z., Knedlik, S., & Loffeld, O. (2010). *Toolbox for GPS-based Attitude Determination: An Implementation Aspect* (pp. 391-395). INTECH Open Access Publisher.

[10] Misra, P., & Enge, P. (2001). *Global positioning system: Signals, measurements, and performance* (2nd ed.). Lincoln, Mass.: Ganga-Jamuna Press.

[11] Kaplan, E., Hegarty, C., Ward, P., & Betz, J. (2006). 5. Satellite Signal Acquisition, Tracking, and Data Demodulation. In *Understanding GPS: Principles and applications* (2nd ed., pp. 153-240). Boston: Artech House.

[12] Ward, Phillip, "The Natural Measurements of a GPS Receiver," *Proceedings of the 51st Annual Meeting of The Institute of Navigation*, Colorado Springs, CO, June 1995, pp. 67-85.

[13] Ward, Phillip W., "Performance Comparisons Between FLL, PLL and a Novel FLL-Assisted-PLL Carrier Tracking Loop Under RF Interference Conditions," *Proceedings of the 11th International Technical Meeting of the Satellite Division of The Institute of Navigation (ION GPS 1998)*, Nashville, TN, September 1998, pp. 783-795.

[14] Ashby, N., & Weiss, M. (1999). Global Position System Receivers and Relativity. In NET Technical Note (Vol. 7385). Boulder, Colorado: National Institute of Standards and Technology.

[15] Wycoff, Eliot, Gao, Grace Xingxin, "A Python Software Platform for Cooperatively Tracking Multiple GPS Receivers," Proceedings of the 27th International Technical Meeting of The Satellite Division of the Institute of Navigation (ION GNSS+ 2014), Tampa, Florida, September 2014, pp. 1417-1425.

[16] Chou, Daniel, Gao, Grace, Xingxin, "Robust GPS-based Timing for PMUs Based on Multi-receiver Position-Information-Aided Vector Tracking," *Proceedings of the 2015 International Technical Meeting of The Institute of Navigation*, Dana Point, CA, January 2015.